P3 type layered oxide frameworks: An appealing family of insertion materials for K-ion batteries

Pawan Kumar Jha, Valérie Pralong, Maximilian Fichtner, Prabeer Barpanda

P3 type layered oxide frameworks: An appealing family of insertion materials for K-ion batteries

Pawan Kumar Jha[1,2], Valérie Pralong[2,3], Maximilian Fichtner[4,5] and Prabeer Barpanda[1,4,5]*

[1] Faraday Materials Laboratory (FaMaL), Materials Research Centre, Indian Institute of Science, Bangalore 560012, India

[2] Normandie University, ENSICAEN, UNICAEN, CNRS, CRISMAT, 14000 Caen, France

[3] Réseau sur le Stockage Electrochimique de l'Énergie (RS2E), Amiens, France

[4] Helmholtz Institute Ulm (HIU), Electrochemical Energy Storage, Ulm 89081, Germany

[5] Institute of Nanotechnology, Karlsruhe Institute of Technology (KIT), Karlsruhe 76021, Germany

Corresponding author: prabeer@iisc.ac.in

Abstract

K-ion batteries (KIBs) offer an efficient technological alternative to the state-of-the-art Li-ion batteries (LIBs) as energy storage devices with similar chemistry, comparable energy densities, elemental economy and uniformly distributed abundant resources. Nonetheless, their practical implementation warrants robust cathode materials that can yield high gravimetric/volumetric energy density, stable cycle life, and high-rate capability. In this scenario, P3 type layered oxides form an appealing family of KIB cathodes, which includes single transition metal based K_xMO_2 (M =transition metals) and multiple transition metals based $K_xMn_{1-y}M_yO_2$. They possess easy and scalable synthesis, high reversible capacity, and adequate operating potential. The current review attempts to capture the most recent advancements in the P3 type KIB cathodes focusing on structural stability, structure-property correlation, and electrochemical performance with suggestions for further material optimization. Finally, the challenges and potential of these P3 type oxide cathodes have been addressed to guide their future research and development as intercalation materials.

Keywords

K-ion batteries, cathodes, Layered oxides, P3 frameworks

1. Introduction

The effective transition from fossil fuels to a carbon-free and sustainable future depends on the advancement of energy storage technologies. The significance of effective and reliable systems for storing energy sporadically produced by renewable resources cannot be overstated. At present, the current state-of-the-art Li-ion battery (LIB) systems propel the consumer electronics, electric vehicles, grid-scale storage and are currently getting increasing deployment in aviation sector [1-4]. However, due to the exponential rise in their usage, Li-ion batteries significantly suffer from drawbacks related to low abundance in the earth's crust and sparse supply chains, resulting in a markedly higher price rise. At this juncture, it is important to develop alternate post-Li-ion battery systems with elemental abundance, operational safety, comparable energy densities without any geographic supply chain constraints. One such feasible alternatives to Li-ion batteries is K-ion batteries (KIB) that employ K^+ as an intercalant species instead of Li^+ [5-8]. In principle, KIB can be economically deployed considering the relative abundance of K element in the earth's crust (20000 ppm for K vis-à-vis 20 ppm for Li) and resulting lower cost of K-based precursors (e.g., 1000 USD/ton of K_2CO_3 vis-à-vis 23000 USD/ton of Li_2CO_3). The standard redox potential of K/K^+ (–2.93 V *vs*. the standard hydrogen electrode [SHE]) is equivalent to Li/Li^+ (–3.04 V *vs*. SHE) and is lower than Na/Na^+ (–2.71 V *vs*. SHE), leading to higher operating potential in KIBs. Also, owing to the low stoke radius, K^+ possesses higher mobility in electrolytes as compared to Li^+ or Na^+ [5-7]. Unlike sodium-ion batteries (NIBs), employing KIB is relatively simple as the well-known graphite anode can be readily used. However, identifying suitable cathodes that reversibly (de)intercalate K^+ ions with high capacity, optimum voltage, efficient rate kinetics, and consistent cycle life is a key challenge for the advancement and implementation of KIBs.

K^+ ions can stabilize different structural types than Li^+ and Na^+ ions owing to their larger ionic radius (1.38 Å) in comparison to Li^+ (0.76 Å) and Na^+ (1.02 Å) ions. Accordingly, the respective cathode materials and their working voltages are likely to differ from those for Li^+ and Na^+ analogues. Similar to the LIBs, layered oxide materials form the major type of cathodes for KIBs with organic electrolytes. Because of their high energy density and two-dimensional open frameworks, layered oxide materials can offer fast K^+ migration rendering them viable cathode candidates for potassium-ion batteries [9-11]. Especially, P3-type layered oxides have gained tremendous attention in the pursuit to develop potential KIB cathode systems [5,12,13]. They (i) can be easily prepared by large-scale (dry) solid-state synthesis, (ii) offer high K^+ ionic conductivity, and (iii) have superior structural integrity than the P2 and O3 counterparts.

Figure 1a depicts a schematic layout of a typical KIB, which includes positive [e.g., P3 $K_{0.5}MO_2$] and negative (e.g., graphite) electrodes with current collectors and electrolyte (e.g., KPF_6 in EC:DEC) soaked separator between the electrodes [5]. The current article overviews the recent advancements in the P3-type K-based cathodes stressing on their structural stability, structure-performance correlation, and overall electrochemical performance. After a sneak peek on mono, binary and ternary transition metal-based oxides, the limitation and potential of these P3 type oxide cathodes have been discussed to offer guidelines for future research and development of these layered insertion materials.

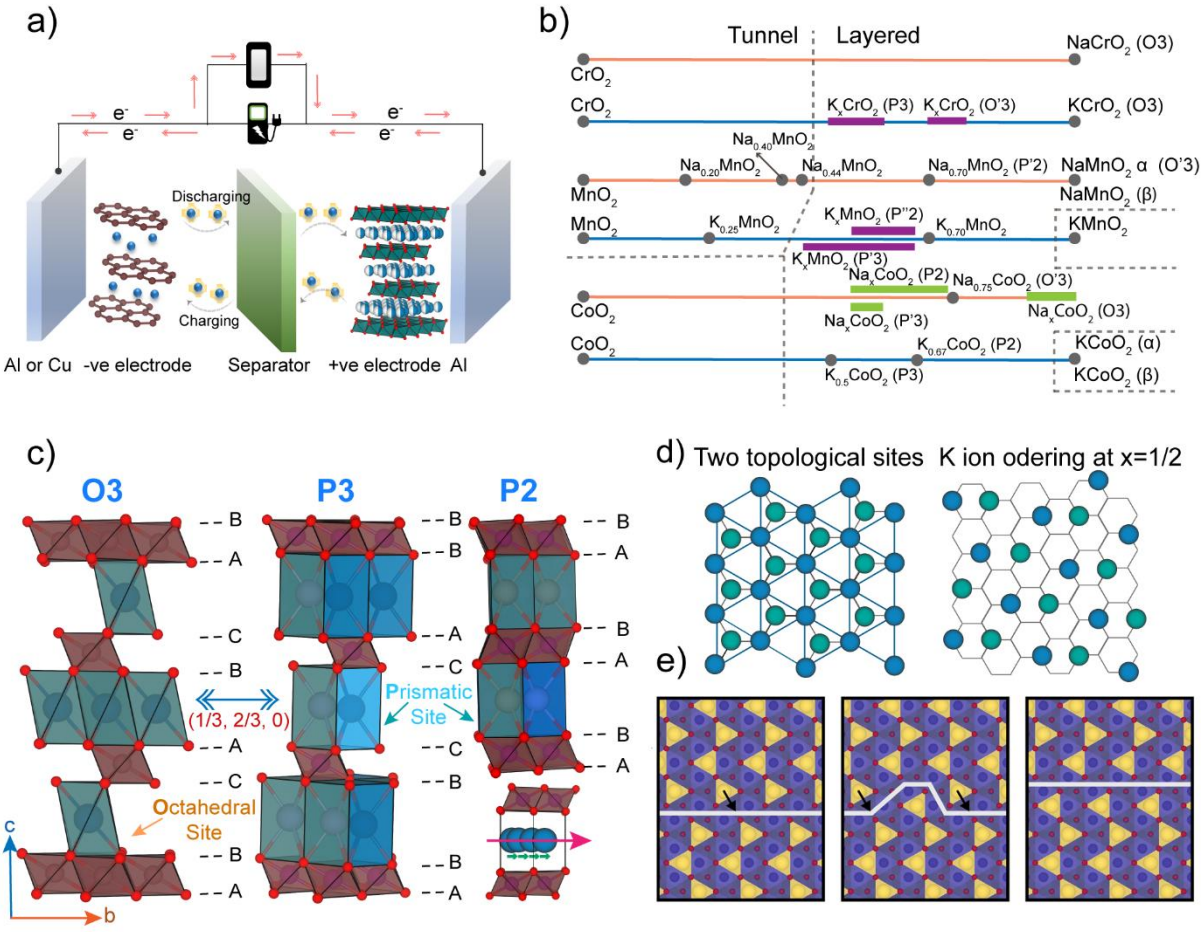

Figure 1. (a) Schematic illustration of operation of typical K^+-ion batteries. **(b)** Phase diagram vs. content of alkali ions (Na and K) as derived by Delmas [10]. **(c)** Schematic illustrations of the O3-, P3-, and P2-frameworks for A_xMO_2 layered oxides. **(d)** Two triangular lattice sites (blue and green balls) available for K^+ ions in P3 structure leading to potential ordering in K-metal layers upon depotassiation [14]. **(e)** Antiphase boundary diffusion mechanism in P3 layered oxides. Arrow marks (black) indicate the migration of antiphase boundary (APB) [15]. Reproduced with permission from Ref. [14-15].

2. Structure stabilization

There are two proposed hypotheses for understanding the favored stacking sequence of anion (oxygen) which determines the type of structure. Based on the critical parameter β (beta) as proposed by Rouxel, the trigonal prismatic environment of alkali-metal ions is preferable at non-stichometry states (K_xMO_2; x<1) [10]. This can be explained by the ionic radius of cation (RK^+ and RM^{3+}/RM^{4+}) and the ionicity of K-O and M^{3+}/M^{4+}–O bonds which are directly correlated to the degree of ionicity or covalence of crystal lattice. The structure stabilization can also be understood from the "cationic potentials" as proposed by Hu group, which expresses the extent of the cation electron density and its polarizability finally normalized to the ionic potential of anion or oxygen [16]. Notably, the P3 type structure is the most stable structure at the intermediate states, as evidenced by the two aforementioned governing parameters and the phase diagram derived by Delmas as presented in **Figure 1b** [10,16].

The structure types (depending on K-vacancy orderings) of layered K_xMO_2, as characterized by the coordination environment and periodicity of MO_2 layer or KO_2 layer in repeated units as reported in the literature, are summarized in **Figure 1c** [10]. It can be defined using an alpha-numeric formulation as proposed by Delmas, with a letter designating the alkali site coordination (ca. octahedral [O] or prismatic [P]) and a number defining the oxygen stacking sequence. The monoclinic distorted O'3-, P'3-, and P'2-type materials are also included with the undistorted types (where ' refers to structural distortion). Notably, the co-existence of several layered stacking suggests the existence of stacking faults as a result of synthesis conditions and/or K^+ (de)intercalation. When M = Sc or Cr, the oxide systems exclusively assume O3-type structure in KMO_2 although they form during the electrochemical (de)charge process [17,18]. $KMnO_2$, on the other hand, has a nonlayered structure composed of chains of [MnO_5] edge-sharing square pyramids [19]. While in $KFeO_2$, tetrahedrally coordinated Fe^{3+} ions are connected through three-dimensional corner sharing fashion [20]. Furthermore, there are numerous reports on the synthesis of P3- (P'3) K_xMO_2 for single transition elements (Cr, Mn, and Co) as well as for mixed transition elements. Owing to the bigger size of K^+-ion and high cation-cation electrostatic repulsion, P3 type stacking is thermodynamically more favored in case of K-based layered oxides [10,21]. Although the P3 structure has twice as many prismatic sites as MO_6 octahedral sites, all prismatic sites cannot be occupied at once due to strong K^+–K^+ electrostatic repulsions, resulting in an ordering of occupied K sites (**Figure 1d**) [14,22-23].

In the P3-type layered structure, all the K^+ ions occupy a single type of prismatic site, sharing a face with an MO_6 octahedron on one side and three edges with surrounding MO_6 octahedra on the opposite side. In the oxygen stacking array AB BC CA along the c-axis, K-metal ions fill the prismatic sites in the inter-slab space between the MO_2 slabs. The (x,y) coordination of oxygen atoms are the same between the interslab space forming a hexagonal unit cell with an R3m or R-3m space group containing three MO_2 slabs. Hexagonal symmetry in the unit cell is obtained when the lattice undergoes monoclinic distortion [10]. To denote distortion, a prime sign is placed between the letter and the number, however, the number of MO_2 slabs is estimated assuming a pseudohexagonal unit cell. For example, the O3-type $KCrO_2$ transforms into O'3-, P3-, and P'3-type K_xCrO_2 during electrochemical K extraction [21]. Notably, P'3-type $K_{0.8}CrO_2$ can be easily synthesized via a simple solid-state reaction [24]. As O3 and P3 share the same space group, it is possible for the O3 phase to transform into the P3 phase by gliding MO_2 slabs by (1/3,2/3,0) without breaking the M-O bond and vice-versa [25,26].

3. Single transition metal-based cathodes

Nonstoichiometric K_xMO_2 oxides crystallize as P3- and P2-type phases, with the K content and calcination temperature having a substantial influence on the final structure type. P3 polymorphs are characterized as low-temperature phase [27]. Indeed, P3-K_xCoO_2 can be synthesized by calcination at a lower temperature than that required for the P2-K_xCoO_2 phase [28]. Furthermore, Delmas et al. reported the synthesis of the P'3- and P'2-types for $x = 0.5$ and $0.55 < x < 0.67$, respectively, by heating a homogenous mixture of K_2O, MnO_2, and Mn_2O_3 in a sealed gold tube at 700 °C [29]. Recent work by Liu et al. reports the P3- and P'2-type phases for $x = 0.45$ and 0.3, respectively, by calcining a K-Mn oxalate coprecipitation precursor at 900 °C in air [30].

The (dis)charge behavior of different polymorphs of K_xMO_2 displayed a lower average voltage of K|| K_xMO_2 than Na_xMO_2 and Li_xMO_2 along with a more inclined (sloping) voltage curve [5]. Goodenough et al. discovered that the electrostatic interaction of the alkali ions in the interslab gap affects the M-O bond length. The stronger electrostatic repulsion leads to the elongation of the M-O bond [31]. As a result, the lower binding energy or lower Madelung stabilization of oxygen with respect to transition metal energy states lead to lower voltage in K_xMO_2 as compared to Li_xCoO_2 and Na_xCoO_2. Further, P3 type intercalation host crystal tends to stabilize cation-vacancy orderings over a wide range of K concentrations negatively

impacting the fast ion transport [14,22,23]. The simplest nearest-neighbor hops in K-vacancy ordered phases are prohibited because they are directed to unstable configurations. Van der Ven group identified an alternative mechanism of K^+ ion transport mediated by antiphase boundary (APB) migration via the formation and expansion of kinks along domain boundaries as displayed in **Figure 1e**. In fact, it relies on extended defects that are inherent to the stable phases rather than vacancy cluster defects and have much lower kinetic barriers for the migration [15,32].

3.1 K_xMnO_2

Mn-based compounds are appealing cathode materials because of the elemental/ precursor abundance. The electrochemical K (de)intercalation performance of layered P3-K_xMnO_2 was first reported by Kim et al. in 2017 [33], whereas its crystal structure was earlier reported by Delmas back in 1976 [29]. The $K_{0.5}MnO_2$, which was synthesized *via* a simple solid-state method, has a rhombohedral lattice with *R*3*m* symmetry exhibiting 140 and 106 $mAhg^{-1}$ capacity in a K-metal half-cell in the voltage range of 1.5-4.2 V and 1.5-3.9 V respectively *vs.* K as presented in **Figure 2a-d**. The narrow operating voltage window yields better cycling stability and retains ~70% (≈70 $mAhg^{-1}$) of the initial discharge capacity with ~95% of coulombic efficiency at a current rate of 20 mAg^{-1} at the end of 50^{th} cycle. *In-situ* XRD measurement suggests the structural transition occurred from P3 to O3 type stacking *via* two-phase mechanism ($0.425<x<0.395$) and further transforms from O3 to an unknown phase (O-3 like) via two-phase reaction ($0.364<x<0.316$) (**Figure 2e-f**) [33]. Notably, the irreversible transition metal migration from the slab to the interslab is less favorable as the interslab distance of K_xMnO_2 monotonically increases during the complete charge process. Less stepwise voltage curve (irreversible) and intensity weakening of (*00l*) peak at higher voltage (4.2 V) during K-removal suggest the stacking fault and other defect induction in a lattice, responsible for the capacity fading during cycling. The discharge process reversibly traces the charging process and indicates feasible K^+ ion (de)insertion from the K_xMnO_2 host. In addition, van der Wall corrected DFT calculations were also in sync with the experimental phase transformation during the (de)insertion process (**Figure 2f**). Even if the upper cut-off voltage is set to a lower value, the capacity fade cannot be avoided entirely [30,33]. Similar to most Mn-based systems, K_xMnO_2 suffers from two significant flaws: the inevitable Jahn-Teller distortion and Mn^{3+} disproportionation ($2Mn^{3+} \rightarrow Mn^{2+} + Mn^{4+}$), which significantly reduce the cycling stability. While the former triggers an asymmetric elongation in the bond lengths of Mn–O in [MnO_6] octahedra, the latter leads to the dissolution of Mn^{2+} into electrolytes. To

address these concerns, recent research suggests that tunable interfacial structure and the induction of a synergistic interaction between particle size, shape, and hollow interior can alleviate structural stress and further provide a shorter K^+ diffusion pathway [34].

3.2 K_xCoO_2

Although P3 type K_xCoO_2 compounds have been studied since the 1970s, their electrochemical K^+ (de)intercalation was reported by the Komaba group as shown in **Figure 2g-h** [28]. The electrochemical properties of K_xCoO_2 follow a similar trend as Na_xCoO_2. Both P2 and P3 phases confirm the comparable capacities of ~60 $mAhg^{-1}$ and 70 $mAhg^{-1}$, respectively having similar voltage profiles in the voltage window of 1.5-3.9 V [28]. A discharge capacity of ≈ 55 $mAhg^{-1}$ or ~92 % of the initial discharge capacity is maintained at the end of 30^{th} cycle by the P3 phase at 11.5 mAg^{-1} rate. The small ionic size (Shannon radius) of Co leads to higher ionic potential of Co (as explained in the above section). As a result, the larger size of K^+ prefers a wide prismatic interslab space that weakens the K^+–K^+ repulsion (or the interaction of K^+ ions). The favorable stability in the prismatic site for K produces a similar charge-discharge profile for P2 and P3 type K_xCoO_2. Due to the stability of the prismatic site, it is reasonable to infer that the P3 type phase was maintained during the (dis)charge process, which is consistent with DFT predicted results [23]. Notably, the fluctuation in $K_{1-x}CoO_2$ interslab lengths caused by the extraction of large K^+ ions is nearly equivalent to $Na_{1-x}CoO_2$. Even with a small amount of residual potassium, the large potassium ions most likely act as pillars while maintaining the wide interslab distance [28]. Additionally, strong K^+–K^+ repulsion is responsible for the differing site energies for K and vacancy, which further results in the stabilization of the K^+–vacancy ordering at various K-contents and undergo several first-order phase transformation steps during cycling.

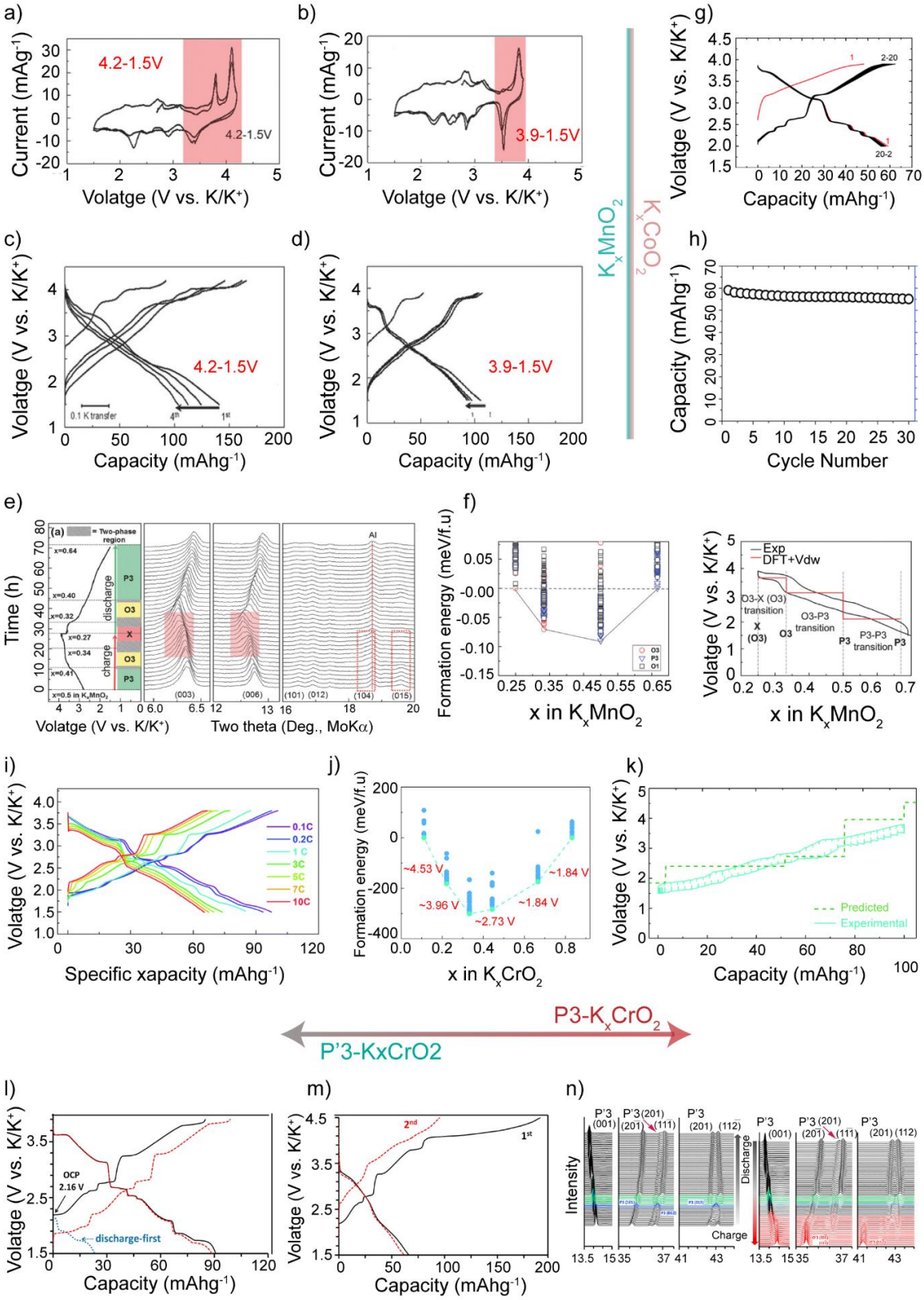

Figure 2. Electrochemical performance of K_xMnO_2 in different potential windows **(a-d)** and phase evolution during cycling from **(e)** *in-situ* XRD study, and **(f)** DFT calculations [33]. **(g-h)** Typical galvanostatic charge and discharge curves and cycling performance of K_xCoO_2 [28]. **(i-k)** Galvanostatic voltage–capacity profiles, convex Hull plot and calculated voltage plot

(DFT) compared to the experimentally obtained charge–discharge profiles for P3 type $KCrO_2$ [35]. (**l-n**) Galvanostatic (dis)charge curves and in-situ XRD patterns of P'3 KxCrO2 synthesized by solid-state method [24].

3.3 K_xCrO_2

As a reasonably abundant element with high electrochemical potential, chromium plays an important role in K-based oxides, which displays all three polymorphs, namely P3, P2, and O3. K-deficient P3 $K_{0.69}CrO_2$ phase was prepared *via* an electrochemical ion-exchange (*chimie douce*) method from parent O3 type $NaCrO_2$ material [35]. While retaining its original crystal structure, the cathode displayed an initial capacity of 100 mAh g^{-1} with reasonable cycling stability (65% capacity retention over 1000 cycles at 1C) as shown in **Figure 2i-k**. Further, P'3 type $K_{0.8}CrO_2$ with the space group *C*2/*m* was prepared using a simple solid-state method as reported by Pyo's group [24]. *In-situ* XRD study revealed that the monoclinic distorted framework was converted into undistorted (or P3 phase) at the intermediate stage of K^+ extraction and this process was completely reversible during subsequent K^+ insertion process as depicted in **Figure 2l-n** [24].

Despite the inherent advantages of unary K_xMO_2 compounds outlined in the preceding section, most of these materials exhibit low capacity, low operating voltage, rapid capacity fading, and several stepwise phase transitions upon charge-discharge process, which limits their practical utility. Fewer voltage steps and smooth voltage curves are desired for the practical applications of K_xMO_2. Based on the experience and knowledge gained from Na_xMO_2 systems [8], fewer voltage steps can be partially obtained in binary, ternary, and quaternary transition-metal systems, as well as by partial substitution with redox inactive metals.

4. Mixed transition metal-based cathodes

4.1 Binary oxides (K_xM1M2O_2)

Mn(M1)/M2-based layered oxides combine the large specific capacity of $Mn^{4+}/M2^{3+}$and the high operating voltage of M2 (=Fe, Co, and Ni). The presence of M2 forms an efficient strategy to suppress the strong cooperative Jahn-Teller distortion associated with high-spin Mn^{3+} ($3d^4$) species. Thus, structural instability during (de)potassiation can be efficiently avoided even with a small amount of M2 substitutions. However, higher Co substitution can result in poor cycling

performance and rate capability associated with first-order phase transition occurring by simply gliding the MO_2 layer (**Figure 3a-d**) [36-39]. Furthermore, increasing the K-content leads to a smoother voltage curve and improved structural stability. Doping of Co greater than x= 0.5 results in lower capacity, even with a K-content of 0.48 per formula unit [37]. On the other hand, Ni substitution enables the multi-electron redox reaction in addition to high voltage, giving rise to energy density. Despite this, the lattice parameter, particularly along the c-axis, varies slightly in $K_{0.5}Ni_{0.1}Mn_{0.9}O_2$ as Ni substitution can reduce the anisotropic change of the Mn–O bond along the c-axis in MnO_6 octahedra (**Figure 3e-h**) [40]. Inherent Ni comes up with a small amount of NiO as an impurity owing to limited solubility and thermodynamic stability of the NiO compound [8]. Noticeably, the electrochemical K^+ intercalation capabilities of K_xMO_2 can be altered by substitution of redox-inactive metals such as Mg, Cu, and Zn. Since the K^+–K^+ electrostatic repulsion is higher than that of Li^+–Li^+ and Na^+–Na^+ species, these metals can successfully accommodate in the MO_2 slab [41,42]. Even though Ni, Co or Mg/Mn-based oxides exhibit promising K^+ storage ability at useful working potentials (**Figure 3 i-k**), a more profound comprehension of phase evolution and a practical structural design suitable for these materials is still notably missing.

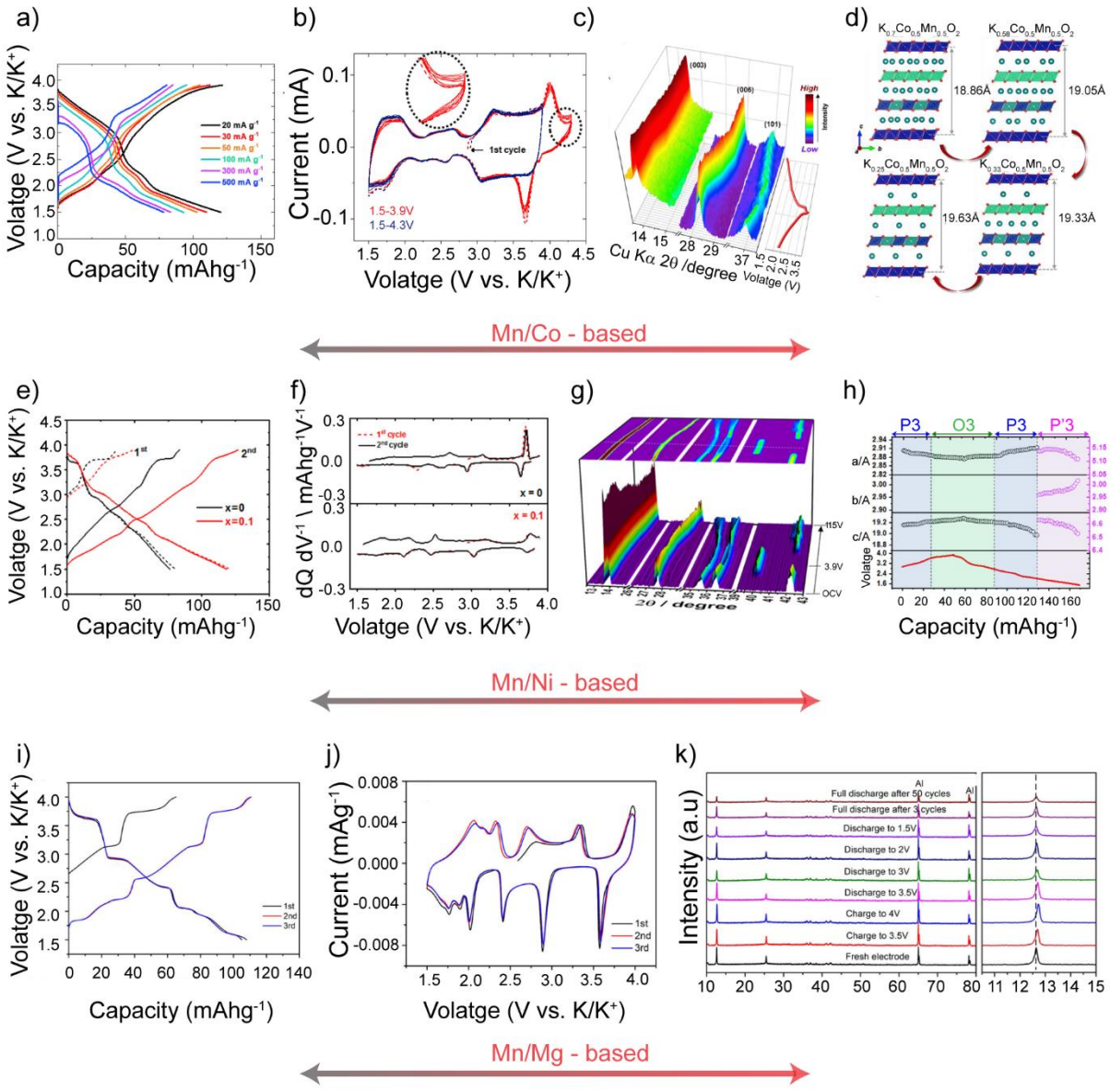

Figure 3. (a) Typical galvanostatic (dis)charge profiles of P3-$K_x[Co_{0.5}Mn_{0.5}]O_2$ on K^+ (de)insertion, corresponding **(b)** cyclic voltammetry plots and **(c)** *operando* XRD phase evolution during cycling revealing **(d)** the change in c-lattice parameter [36]. **(e)** Galvanostatic (dis)charge profiles of $K_{0.5}Ni_{0.1}Mn_{0.9}O_2$, **(f)** corresponding dQ/dV curves and **(g-h)** *operando* XRD patterns during cell cycling [40]. **(i)** Galvanostatic (dis)charge profiles, and respective **(j)** cyclic voltammogram and (k) ex situ XRD patterns for Mg-doped K_xMnO_2 [42].

4.2 Ternary oxides ($K_xM1M2M3O_2$)

The drawbacks of the Mn-based layered cathode materials, such as low voltage, structural and capacity degradation, can be partially solved by replacing Mn^{3+} with Fe^{3+}, Mg^{2+} and Ni^{2+} [43-

45]. For example, ternary $K_{0.5}Mn_{0.8}Fe_{0.1}Ni_{0.1}O_2$ oxide has a high reversible discharge capacity (120 mAh g^{-1}) involving P3–O3 phase transition along with good structural integrity over 300 cycles (74% capacity retention) at 50 mA g^{-1} (**Figure 4a-c**). It could be attributed to slight structural variation and facile migration of K^+ ions. From a structural standpoint, the shared oxygen atoms in MnO_6, FeO_6, and NiO_6 (O–Mn–O–Fe–O–Ni–O) could preclude the introduction of structural defects like the Jahn-Teller phenomenon in MnO_6 octahedra. Conversely, P3-type ternary $K_{0.67}Ni_{0.17}Co_{0.17}Mn_{0.66}O_2$ oxide delivers a discharge capacity of 77 $mAhg^{-1}$ in the range 4.3-2 V with a lower interslab distance as evidenced by ex situ XRD patterns after charging to 4.3 V (**Figure 4d-f**).

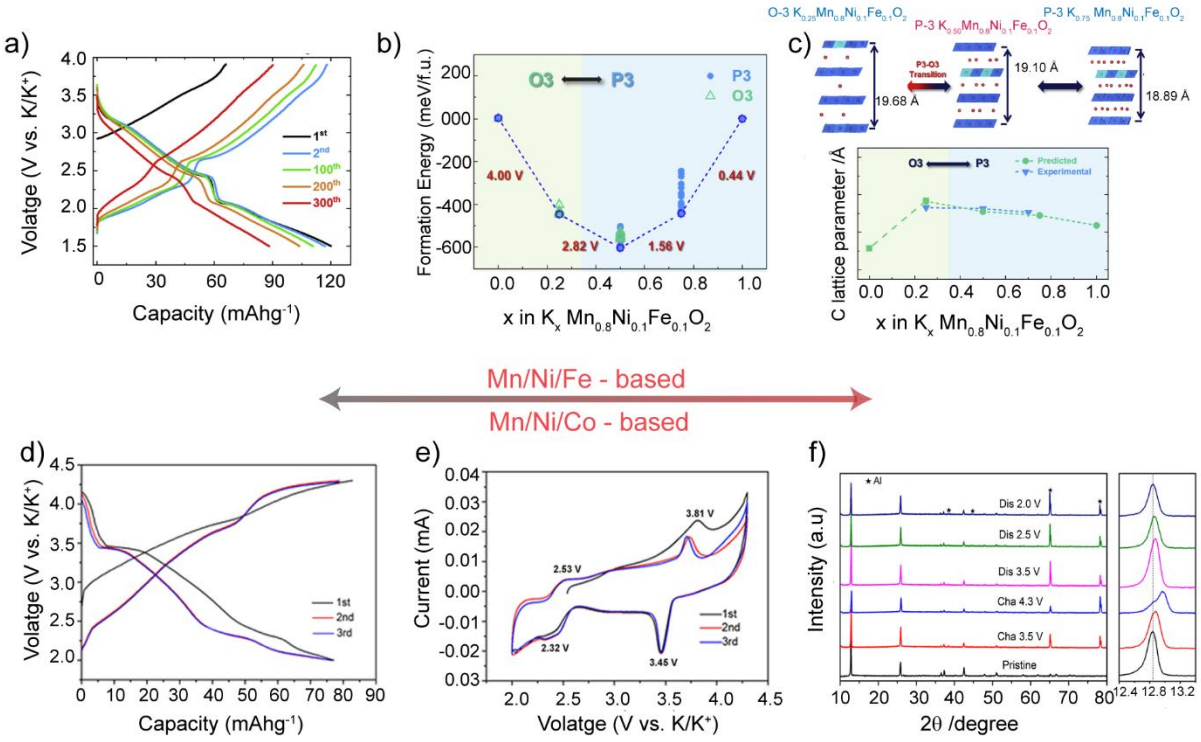

Figure 4 (a) Galvanostatic (dis)charge profiles of $K_{0.5}Mn_{0.8}Fe_{0.1}Ni_{0.1}O_2$ oxide, **(b)** DFT calculations-based formation energy plot depicting the structural evolution in of $K_{0.5}Mn_{0.8}Fe_{0.1}Ni_{0.1}O_2$ in a K-half cell. The formation energies are normalized per formula unit. **(c)** Corresponding evolution of phases and lattice parameter c during K^+ (de)insertion [43]. **(d)** Galvanostatic (dis)charge curves of P3 $K_{0.67}Ni_{0.17}Co_{0.17}Mn_{0.66}O_2$, corresponding **(e)** dQ/dV profiles, and **(f)** ex situ XRD patterns during the first cycle in a K-half cell [44].

5. Conclusion and perspectives

P3-type layered oxides and their derivatives form a promising group of cathode insertion materials for advanced potassium-ion batteries (KIBs) aimed at large-scale energy storage. In recent years, significant progress has been achieved in harnessing these P3 oxide cathodes, but there are still numerous concerns that must be addressed before KIBs can be realized in the future. The low coulombic efficiency, chemical stability, K-deficiency, lower voltage owing to strong K^+–K^+ repulsion, and several first-order phase transformations (including guiding) or K^+/vacancy ordering results in a stepwise voltage profile. Along this line, coating the active layer can be a viable solution in achieving chemical stability since it improves rate capability and cycling stability by mitigating side reactions at the electrode interface. The proper selection of cation substituents with large ionic radius should be beneficial to accommodate more K^+ in pristine layer structure. The presence of larger transition metal (M) leads to higher lattice parameters, thereby favoring the introduction of larger cations and stabilization of pristine layered structure with higher K^+ content, which in turn is beneficial to yield higher capacity. For instance, if the charge ordering of M layers in K_xMO_2 is disrupted, the K^+/vacancy ordering could be effectively avoided. Slight differences in the ionic radii of different dopants and significant differences in the redox potentials are conducive to form disordered configurations. Moreover, high entropy P3 type oxides made up of several transition metals might exhibit greater cycling stability and higher capacity, as reported in case of sodium-ion batteries. Another technique to improve battery performance can be tweaking the particle size, shape, and morphology. Caution must be exercised during materials handling as K-based compounds have lower moisture stability than Na and Li counterparts as they can accommodate crystal water when exposed to open air. Poor moisture stability can affect the cycling performance and rate performance necessitating careful storage and handling conditions. We anticipate this review offers fresh perspectives for further development of P3-type layered oxide cathodes for rechargeable potassium-ion batteries.

Declaration of competing interest

The authors declare that they have no known competing financial interests or personal relationships that could have appeared to influence the work reported in this paper.

Acknowledgements

The first author is grateful to the Ministry of Human Resource Development (MHRD, Government of India) for graduate fellowship. PKJ, VP and PB acknowledge the Indian-French Laboratory of Solid State Chemistry (LaFICS) for financial support. The work was partially funded by the Deutsche Forschungsgemeinschaft (DFG, German Research Foundation) under Germany´s Excellence Strategy – EXC 2154 – Project number 390874152. It also contributes to the research performed at CELEST (Center for Electrochemical Energy Storage Ulm-Karlsruhe) and was funded by the German Research Foundation (DFG) under Project ID 390874152 (POLiS Cluster of Excellence). PB is grateful to the Alexander von Humboldt Foundation (Bonn, Germany) for a 2022 Humboldt fellowship for experienced researchers.

CRediT author statement

Pawan Kumar Jha: Conceptualization, Writing- Original draft preparation. **Valerie Pralong, Maximilian Fichtner, Prabeer Barpanda**: Supervision, Writing- Reviewing and Editing.

References

1. Armand M, Tarascon JM: **Building better batteries**. *Nature* 2008, **451**:652-657.
2. Dunn B, Kamath H, Tarascon J-M: **Electrical energy storage for the grid: A battery of choices**. *Science* 2011, **334**:928-935.
3. Whittingham MS: **History, evolution, and future status of energy storage**. *Proc. IEEE* 2012, **100**:1518-1534.
4. Whittingham MS: **Ultimate limits to intercalation reactions for lithium batteries**. *Chem. Rev.* 2014, **114**:11414-11443.
5. Hosaka T, Kubota K, Hameed AS, Komaba S: **Research development on K-ion batteries**. *Chem. Rev.* 2020, **120**:6358-6466.
** This is the comprehensive review report on K-ion batteries (KIBs).
6. Hwang J-Y, Myung S-T, Sun Y-K: **Recent progress in rechargeable potassium batteries**. *Adv. Funct. Mater.* 2018, **28**:1802938.
7. Kim H, Kim JC, Bianchini M, Seo D-H, Rodriguez-Garcia J, Ceder G: **Recent progress and perspective in electrode materials for K-ion batteries**. *Adv. Energy Mater.* 2018, **8**:1702384.
8. Yabuuchi N, Kubota K, Dahbi M, Komaba S: **Research development on sodium-ion batteries**. *Chem. Rev.* 2014, **114**:11636-11682.
9. Delmas C, Fouassier C, Hagenmuller P: **Evolution cristallochimique et propriétés physiques de quelques oxydes lamellaires**. *Mater. Sci. Engg.* 1977, **31**:297-301.

10. Delmas C, Fouassier C, Hagenmuller P: **Structural classification and properties of the layered oxides**. *Physica B+C* 1980, **99**:81-85.
* The general nomenclature of layered oxides is given along with the phase diagram of K (and Na) with different trainsition elements.
11. Fouassier C, Delmas C, Hagenmuller P: **Evolution structurale et proprietes physiques des phases A_xMO_2 (A = Na, K; M = Cr, Mn, Co) ($x \leqslant 1$)**. *Mater. Res. Bull.* 1975, **10**:443-449.
12. Zhang X, Wei Z, Dinh KN, Chen N, Chen G, Du F, Yan Q: **Layered oxide cathode for potassium-ion battery: Recent progress and prospective**. *Small.* 2020, **16**:2002700.
13. Kim H, Ji H, Wang J, Ceder G: **Next-generation cathode materials for non-aqueous potassium-ion batteries**. *Trends Chem.* 2019, **1**:682-692.
14. Kaufman JL, Van der Ven A: **Ordering and structural transformations in layered K_xCrO_2 for K-ion batteries**. *Chem. Mater.* 2020, **32**:6392-6400.
* The authors report the zig-zag row ordering of K-ions in P3 type layered oxide systems. Thermodynamic phase transformation upon (de)charge has been evaluted using DFT calculations.
15. Kaufman JL, Van der Ven A: **Antiphase boundary migration as a diffusion mechanism in a P3 sodium layered oxide.** *Phys. Rev. Mater.* 2021, **5**:055401.
** Antiphase boundary diffusion (APB) mechanism in P3-type layered oxide is discussed in detail.
16. Zhao C, Wang Q, Yao Z, Wang J, Sánchez-Lengeling B, Ding F, Qi X, Lu Y, Bai X, Li B, et al.: **Rational design of layered oxide materials for sodium-ion batteries**. *Science*. 2020, **370**:708-711.
17. Delmas C, Devalette M, Fouassier C, Hagenmuller P: **Les phases K_xCrO_2 ($x \leqslant 1$)**. *Mater. Res. Bull.* 1975, **10**:393-398.
18. Hoppe R, Sabrowsky H: **Oxoscandate der alkalimetalle: $KScO_2$ und $RbScO_2$**. *Z. Anorg. Allg. Chem.* 1965, **339**:144-154.
19. Jansen M, Chang FM, Hoppe R: **Zur kenntnis von $KMnO_2$**. *Z. Anorg. Allg. Chem.*1982, **490**:101-110.
20. Han SC, Park WB, Sohn K-S, Pyo M: **$KFeO_2$ with corner-shared FeO_4 frameworks as a new type of cathode material in potassium-ion batteries**. *J. Solid State Electrochem.* 2019, **23**:3135-3143.
21. Kim H, Seo D-H, Urban A, Lee J, Kwon D-H, Bo S-H, Shi T, Papp JK, McCloskey BD, Ceder G: **Stoichiometric layered potassium transition metal oxide for rechargeable potassium batteries**. *Chem. Mater.* 2018, **30**:6532-6539.
* This paper explores the preferred codination of different transition metals in K-based systems.
22. Kaufman JL, Van der Ven A: **Na_xCoO_2 phase stability and hierarchical orderings in the O3/P3 structure family**. *Phys. Rev. Mater.* 2019, **3**:015402.
23. Toriyama MY, Kaufman JL, Van der Ven A: **Potassium ordering and structural phase stability in layered K_xCoO_2**. *ACS Appl. Energy Mater.* 2019, **2**:2629-2636.
24. Naveen N, Han SC, Singh SP, Ahn D, Sohn K-S, Pyo M: **Highly stable P′3-$K_{0.8}CrO_2$ cathode with limited dimensional changes for potassium ion batteries**. *J. Power Sources* 2019, **430**:137-144.
25. Komaba S, Yabuuchi N, Nakayama T, Ogata A, Ishikawa T, Nakai I: **Study on the reversible electrode reaction of $Na_{1-x}Ni_{0.5}Mn_{0.5}O_2$ for a rechargeable sodium-ion battery**. *Inorg. Chem.* 2012, **51**:6211-6220.
26. Kubota K, Kumakura S, Yoda Y, Kuroki K, Komaba S: **Electrochemistry and solid-state chemistry of $NaMeO_2$ (Me = 3d Transition Metals)**. *Adv. Energy Mater.* 2018, **8**:1703415.

27. Paulsen JM, Dahn JR: **O2-type $Li_{2/3}[Ni_{1/3}Mn_{2/3}]O_2$: A new layered cathode material for rechargeable lithium batteries II. Structure, composition, and properties**. *J. Electrochem. Soc.* 2000, **147**:2478.
28. Hironaka Y, Kubota K, Komaba S: **P2- and P3-K_xCoO_2 as an electrochemical potassium intercalation host**. *Chem. Commun.* 2017, **53**:3693-3696.
29. Delmas C, Fouassier C: Les Phases K_xMnO_2 ($x \leq 1$). *Z. Anorg. Allg. Chem.* 1976, **420**:184-192.
30. Liu C-l, Luo S-h, Huang H-b, Zhai Y-c, Wang Z-w: **Layered potassium-deficient P2- and P3-type cathode materials K_xMnO_2 for K-ion batteries**. *Chem. Eng. J.* 2019, **356**:53-59.
31. Goodenough JB, Mizushima K, Takeda T: **Solid-solution oxides for storage-Battery electrodes**. *Jpn. J. Appl. Phys.* 1980, **19**:305.
32. Kaufman JL, Van der Ven A: **Cation diffusion facilitated by antiphase boundaries in layered intercalation compounds**. *Chem. Mater.* 2022, **34**:1889-1896.
33. Kim H, Seo D-H, Kim JC, Bo S-H, Liu L, Shi T, Ceder G: **Investigation of potassium storage in layered P3-type $K_{0.5}MnO_2$ cathode**. *Adv. Mater.* 2017, **29**:1702480.
* This paper explores the P3 type $K_{0.5}MnO_2$ as a positive insertion host for KIBs. The electrochemical studies has been performed and stable voltage window as well as the phase transition during cycling has been analysed.
34. Lei K, Zhu Z, Yin Z, Yan P, Li F, Chen J: **Dual interphase layers in situ formed on a manganese-based oxide cathode enable stable potassium storage**. *Chem.* 2019, **5**:3220-3231.
35. Hwang J-Y, Kim J, Yu T-Y, Myung S-T, Sun Y-K: **Development of P3-$K_{0.69}CrO_2$ as an ultra-high-performance cathode material for K-ion batteries**. *Energy Environ. Sci.* 2018, **11**:2821-2827.
36. Choi JU, Kim J, Hwang J-Y, Jo JH, Sun Y-K, Myung S-T: **$K_{0.54}[Co_{0.5}Mn_{0.5}]O_2$: New cathode with high power capability for potassium-ion batteries**. *Nano Energy* 2019, **61**:284-294.
37. Sada K, Barpanda P: **P3-type layered $K_{0.48}Mn_{0.4}Co_{0.6}O_2$: a novel cathode material for potassium-ion batteries**. *Chem. Commun.* 2020, **56**:2272-2275.
38. Ramasamy HV, Senthilkumar B, Barpanda P, Lee Y-S: **Superior potassium-ion hybrid capacitor based on novel P3-type layered $K_{0.45}Mn_{0.5}Co_{0.5}O_2$ as high capacity cathode**. *Chem. Eng. J.* 2019, **368**:235-243.
39. Zhang Q, Didier C, Pang WK, Liu Y, Wang Z, Li S, Peterson VK, Mao J, Guo Z: **Structural insight into layer gliding and lattice distortion in layered manganese oxide electrodes for potassium-ion batteries**. *Adv. Energy Mater.* 2019, **9**:1900568.
40. Cho MK, Jo JH, Choi JU, Myung S-T: **Cycling stability of layered potassium manganese oxide in nonaqueous potassium cells**. *ACS Appl. Mater. Interfaces* 2019, **11**:27770-27779.
41. Weng J, Duan J, Sun C, Liu P, Li A, Zhou P, Zhou J: **Construction of hierarchical $K_{0.7}Mn_{0.7}Mg_{0.3}O_2$ microparticles as high capacity & long cycle life cathode materials for low-cost potassium-ion batteries**. *Chem. Eng. J.* 2020, **392**:123649.
42. Liu C-L, Luo S-H, Huang H-B, Zhai Y-C, Wang Z-W: **Low-cost layered $K_{0.45}Mn_{0.9}Mg_{0.1}O_2$ as a high-performance cathode material for K-ion batteries**. *ChemElectroChem.* 2019, **6**:2308-2315.
43. Choi JU, Kim J, Jo JH, Kim HJ, Jung YH, Ahn D-C, Sun Y-K, Myung S-T: **Facile migration of potassium ions in a ternary P3-type $K_{0.5}[Mn_{0.8}Fe_{0.1}Ni_{0.1}]O_2$ cathode in rechargeable potassium batteries**. *Energy Storage Mater.* 2020, **25**:714-723.

44. Liu C, Luo S, Huang H, Wang Z, Hao A, Zhai Y, Wang Z: **$K_{0.67}Ni_{0.17}Co_{0.17}Mn_{0.66}O_2$: A cathode material for potassium-ion battery**. *Electrochem. Commun.* 2017, **82**:150-154.
45. Liu L, Liang J, Wang W, Han C, Xia Q, Ke X, Liu J, Gu Q, Shi Z, Chou S, et al.: **A P3-type $K_{1/2}Mn_{5/6}Mg_{1/12}Ni_{1/12}O_2$ cathode material for potassium-ion batteries with high structural reversibility secured by the Mg–Ni pinning effect**. *ACS Appl. Mater. Interfaces* 2021, **13**:28369-28377.